Many-body effects on the cyclotron resonance in a two-dimensional electron gas

C. Kallin* and B. I. Halperin
Department of Physics, Harvard University, Cambridge, Massachusetts 02138
(Received 20 August 1984)

We consider optical absorption by an interacting two-dimensional electron system, with impurities, in a strong perpendicular magnetic field, at electron densities such that an integral number of Landau levels is filled. The Coulomb energy $e^2/\epsilon l_0$ is assumed to be smaller than the cyclotron energy $\hbar\omega_c$, and correlation effects are treated exactly to lowest order in $(e^2/\epsilon l_0)/\hbar\omega_c$. The impurity scattering is treated in a self-consistent approximation for several different impurity potentials. The cyclotron resonance line is found to be significantly altered by electron-electron interactions. The line is shifted to lower frequencies and a line narrowing due to correlation effects is found.

I. INTRODUCTION

Two-dimensional electron systems, such as occur in the inversion layers of metal-oxide-semiconductor field-effect transistors (MOSFET's) and GaAs-$Al_xGa_{1-x}As$ heterojunctions at low temperatures, are particularly interesting systems in which to study many-body effects.[1] This is because the electron density, and hence the relative strength of the Coulomb interaction, can be experimentally varied over a wide range and, at least in the heterojunctions, the effect of impurities is often very small. In addition, correlation effects are typically stronger in two dimensions than in three dimensions, and the theoretical analysis is often simpler. In this paper we will investigate many-body effects in optical absorption by a disordered two-dimensional electron gas (2D EG), in a strong perpendicular magnetic field.

Considerable work has been done on cyclotron resonance in two-dimensional electron systems. Early theoretical investigations neglected electron-electron interactions and focused on the effects of disorder and impurity scattering.[2–5] The energy spectrum of an ideal 2D EG is discrete and, because of this singular nature, broadening effects must be treated self-consistently. The frequency-dependent conductivity of a disordered, but noninteracting, 2D EG in a perpendicular magnetic field has been studied in detail for various kinds of scatterers. The scatterers have been treated in the self-consistent Born approximation (SCBA),[2] which is the simplest treatment that is free from divergences, as well as in higher-order self-consistent approximations.[3]

While these theories do give reasonable agreement with some cyclotron resonance experiments,[6] many observed features of the resonance cannot be explained by such theories. For example, the occurrence of relatively strong harmonics which are shifted from exact integral multiples of the fundamental cyclotron resonance,[7–9] linewidth narrowing in very strong magnetic fields when only the lowest Landau level is occupied,[10,11] and linewidth broadening[11–14] or splitting[14] at certain filling factors or electron densities, have all been attributed to many-body effects, although only the first of these phenomena is well understood.[8,9]

It is well known that in a system with translational symmetry, the cyclotron resonance line shape is unaffected by electron-electron interactions.[15] However, the presence of impurities allows coupling to magnetoplasma modes at nonzero wave vector, where correlation effects are important. The optical-absorption spectra will then be affected by the dispersion of the magnetoplasma modes. Therefore, to study many-body effects one must treat electron-electron and electron-impurity interactions together. This has typically been done by treating electron-electron—interaction effects in the random-phase approximation (RPA) and electron-impurity scattering in lowest-order perturbation theory,[9] using a memory-function approach.[16,17] However, for strong magnetic fields the RPA is not accurate at large wave vectors.[18] In addition, such an approach results in unphysical divergences in the absorption spectra because the broadening of the excitation spectrum in the intermediate states, arising from electron-impurity scattering, is not included in this approximation. In the work of Ting, Ying, and Quinn,[9] broadening due to impurities was included in the analysis by introducing the experimentally measured transport lifetime as a single-particle lifetime. While such an approach may be reasonable for silicon inversion layers, where the scatterers are predominantly short ranged, it is not valid for high-mobility heterojunctions, where the dominant scattering mechanism is long-range Coulomb scattering.[19,20] For this scattering mechanism, Das Sarma and Stern[21] have pointed out that the single-particle lifetime may be several orders of magnitude smaller than the transport lifetime. In any case, one would like to treat the broadening in a self-consistent way, which includes vertex corrections as well as self-energy corrections.

Fukuyama, Kuramoto, and Platzman[22] went beyond the RPA, but also treated electron-impurity scattering to lowest order. In their analysis they considered the strong-magnetic-field and long-wavelength limits, at relatively high temperatures, and at filling factors less than 1. In that case the excitation spectrum is broadened due to electron-electron interactions.[23]

Schlesinger *et al.* considered a model, involving coupling between the cyclotron mode and finite-wavelength magnetoplasmons, to explain the experimental observation

of linewidth broadening and splitting at certain electron densities.[14] They made an *ad hoc* assumption for the corrections to the RPA energy spectrum and for the broadening due to impurities. By varying parameters they were able to obtain a reasonable fit to the experimental data. In their model one obtains two peaks in the absorption spectra (or a splitting of the cyclotron peak) when finite-wave-vector magnetoplasmons are shifted into resonance with the cyclotron mode.

In the present paper we take a different approach than previous investigations of many-body effects on the cyclotron resonance. We restrict our analysis to the case where the electron density and magnetic field are such that an integral number of Landau levels are filled. We also assume that the magnetic field is sufficiently strong, so that the cyclotron energy $\omega_c = eB/m^*c$ is larger than the Coulomb energy $E_{Co} \equiv e^2/\epsilon l_0$, where ϵ is the background dielectric constant and $l_0 = (c/eB)^{1/2}$ is the magnetic length. (We set $\hbar = 1$.) In addition, we assume that the thermal energy $k_B T$ is much smaller than ω_c, so that we can work at zero temperature.

We make the restriction to completely filled Landau levels for the sake of its theoretical simplicity. This restriction allows us to treat the effect of electron-electron interactions exactly to order $e^2/\epsilon l_0$. Moreover, in this case there is no broadening of the excitation spectrum in the absence of impurities,[9] and no screening by the electrons to lowest order in E_{Co}/ω_c.[13] Of course, experiments are done at both integer and noninteger filling factors. It is an open question, theoretically and experimentally, whether there should be a strong variation in the cyclotron resonance as one passes from integer to noninteger filling factor.[11–14]

In an earlier paper we calculated the density response function of our model in the absence of disorder.[18] The elementary neutral excitations near ω_c may be described as magnetoplasma modes, or "magnetic excitons" in which one electron is excited to an unoccupied Landau level n, leaving behind a hole in a filled Landau level $n-1$. The energy of the magnetic exciton is the kinetic-energy difference ω_c plus an energy shift, due to electron-electron interactions, which is of order $e^2/\epsilon l_0$. (This energy spectrum was first calculated by Bychkov, Iordanskii, and Éliashberg, for the case of one spin state occupied in the lowest Landau level;[24] the dispersion was derived in Ref. 18 for other integral filling factors.) These exciton states are a complete set of states for excitations near ω_c. In the presence of disorder we use these exciton states as a basis, and consider the scattering of excitons by impurities. The impurity scattering is treated self-consistently, in an approximation which neglects multiple scattering from a single impurity and neglects most correlation effects between impurities. We assume that the impurity scattering is sufficiently weak and the impurity concentration is sufficiently small that such an approximation is valid. This approximation is at least sensible for arbitrary ratios of the strength of electron-impurity scattering to electron-electron scattering. Moreover, it is, in fact, exact in the weak electron-impurity—scattering limit. We will refer to this approximation as the self-consistent exciton approximation (SCEA).[25]

The model and impurity potentials we consider are described in Sec. II below. An expression for the conductivity is also given in this section. In Sec. III we review some properties of the pure system which are used in this paper. The relevant magnetic exciton energies and wave functions are given here. The optical-absorption spectra of the disordered system are investigated in Secs. IV and V. Impurity scattering is treated to lowest order in Sec. IV, and is treated self-consistently in Sec. V. The results of the self-consistent calculation are discussed in Sec. VI and the conclusions are presented in Sec. VII.

We find that electron-electron interactions are important in the high-magnetic-field limit. At integer filling factors, correlation effects narrow the cyclotron resonance peak and shift it to lower frequency. We find line shapes which are in qualitative agreement with experiments on high-mobility GaAs heterojunctions, if we assume that the impurity potential is long ranged. If one assumes short-range scatterers, however, the peak is narrowed even more, giving linewidths (for high-mobility samples) that are much smaller than the experimental widths. For a given mobility, the cyclotron linewidth is much larger for long-range scatterers than for short-range scatterers because long-range scatterers are relatively ineffective in reducing the mobility.[21]

We expect our analysis to be more applicable to GaAs heterojunctions than to Si inversion layers for several reasons: (1) The assumption of moderate disorder is more likely to be satisfied in the high-mobility heterojunctions, (2) the high-field limit is more accessible in GaAs because of the smaller effective mass, and (3) there is a valley degeneracy in the Si inversion layers which we have not taken into account. (The valley degeneracy will increase the density of exciton states at ω_c, which we believe will probably reduce the effects of electron-electron interactions.) For these reasons we have concentrated on impurity potentials which are reasonable models for scattering in GaAs heterojunctions.

II. MODEL AND THE DYNAMICAL CONDUCTIVITY

A. Model and impurity potential

We consider a two-dimensional electron gas, at zero temperature, in a perpendicular magnetic field $\mathbf{B} = B_0 \hat{\mathbf{z}}$, which is described by the Hamiltonian

$$\mathscr{H} = \mathscr{H}_0 + \mathscr{H}_{e\text{-}e} + \mathscr{H}_{e\text{-}i} , \tag{2.1a}$$

where

$$\mathscr{H}_0 = \frac{1}{2m^*} \sum_i (\mathbf{p}_i - e\mathbf{A}_i/c)^2 + g\mu_B \sum_i \mathbf{B}\cdot\mathbf{S}_i , \tag{2.1b}$$

$$\mathscr{H}_{e\text{-}e} = \sum_{i<j} v(\mathbf{r}_i - \mathbf{r}_j) - \frac{Nn_e}{2} \int d\mathbf{r}\, v(\mathbf{r}) , \tag{2.1c}$$

$$\mathscr{H}_{e\text{-}i} = \sum_{i,k} u(\mathbf{r}_i - \mathbf{R}_k, Z_k) , \tag{2.1d}$$

$n_e = N/A$, N is the number of electrons, and A is the area of the system. $\mathscr{H}_0$ includes the kinetic energy and Zeeman energy, $\mathscr{H}_{e\text{-}e}$ describes the interaction between elec-

trons, with $v(r)=e^2/\epsilon r$, and the interaction with the positive background. The interaction with the impurities is described by $\mathscr{H}_{e\text{-}i}$, where $u(\mathbf{r}-\mathbf{R}_k,Z_k)$ is the effective potential of an impurity located at $(\mathbf{R}_k,Z_k)$. We work in the Landau gauge, so that the vector potential, at the ith electron, is $\mathbf{A}_i\equiv\mathbf{A}(\mathbf{r}_i)=B_0 y_i\hat{\mathbf{x}}$. In addition, we assume that the magnetic field and electron density are such, that for $v=u=0$, an integral number of Landau levels are filled. The magnetic field is assumed to be sufficiently strong that the cyclotron energy ω_c is large compared to the Coulomb energy $e^2/\epsilon l_0$ and the random impurity potential.

The impurity potential for GaAs-AlGaAs heterojunctions is not well known. The dominant scattering mechanism is believed to be scattering due to the ionized impurities which are set back from the inversion layer by a minimum distance α, typically several hundred angstroms.[19,20] The impurity potential is assumed to be the Coulomb potential,

$$u(\mathbf{r}-\mathbf{R}_i,Z_i)=\frac{e^2}{\epsilon_I(|\mathbf{r}-\mathbf{R}_i|^2+Z_i^2)^{1/2}}\ , \tag{2.2}$$

where ϵ_I is the dielectric constant of the surrounding medium ($Al_xGa_{1-x}As$). This potential is *not* screened by the electrons in the two-dimensional layer, for the special case of integer filling factors.[13]

For illustrative purposes and comparison, we will also consider the simple case of short-range scatterers, in the inversion layer itself,

$$u(\mathbf{r}-\mathbf{R}_i,Z_i)=\frac{a\hbar^2}{2m^*}\delta(\mathbf{r}-\mathbf{R}_i)\delta_{Z_i,0}\ , \tag{2.3}$$

where a is a dimensionless constant. Also for purposes of illustration, we consider an impurity potential used in Ref. 22 as a model for surface roughness.

B. Dynamical conductivity

The absorption of infrared radiation, normally incident on this system, due to cyclotron resonance, is proportional to the real part of the dynamical conductivity,

$$\sigma_{\alpha\beta}(\omega)=i\frac{\omega_p^2}{4\pi\omega}\delta_{\alpha\beta}+i\frac{Q_{\alpha\beta}(\omega)}{\omega}\quad(\alpha,\beta=x,y)\ . \tag{2.4}$$

Here, $\omega_p^2=4\pi e^2 n_e/m^*$ is the plasma frequency squared, and $Q_{\alpha\beta}$ is the current-current correlation function,

$$Q_{\alpha\beta}(\omega)=-i\int_0^\infty dt\, e^{i\omega t}\langle[j_\alpha(t),j_\beta(0)]\rangle\ , \tag{2.5}$$

where the current operator is

$$\mathbf{j}=\frac{e}{m^*}\sum_i(\mathbf{p}_i-e\mathbf{A}_i/c)\ .$$

It follows from symmetry that $\sigma_{xx}=\sigma_{yy}$, and $\sigma_{xy}=-\sigma_{yx}$. Near ω_c, the absorption is proportional to the real part of $\sigma_+\equiv\sigma_{xx}-i\sigma_{xy}$, which is determined, in turn, by $Q_+\equiv Q_{xx}-iQ_{xy}$.

III. EXCITATIONS OF THE PURE TWO-DIMENSIONAL ELECTRON GAS

In this section we review the properties, derived in our earlier work, of the elementary neutral excitations with energies close to ω_c, for the interacting 2D EG in the absence of impurities.[18] In the strong-magnetic-field limit these excitations may be described as magnetic excitons, as discussed in the Introduction.

A. Magnetic exciton wave functions and energies

If we neglect the spin degree of freedom, the wave function describing an exciton which consists of an electron in the nth Landau level and a hole in the $(n-1)$th Landau level is calculated to be[22]

$$\Psi_{\mathbf{k}n}(\mathbf{R},\Delta\mathbf{r})=\frac{1}{2\pi}e^{i\mathbf{k}\cdot\mathbf{R}}e^{iX\Delta y/l_0^2}\phi_n(\Delta\mathbf{r}-l_0^2\mathbf{k}\times\hat{\mathbf{z}})\ , \tag{3.1a}$$

$$\phi_n(\mathbf{r})\equiv\frac{1}{(2nl_0^2)^{1/2}}e^{-r^2/4l_0^2}\left[\frac{x+iy}{l_0}\right]L_{n-1}^1\left[\frac{r^2}{2l_0^2}\right]\ , \tag{3.1b}$$

in the Landau gauge, where L_n^α is a Laguerre polynomial. Here, $\mathbf{R}\equiv(\mathbf{r}_1+\mathbf{r}_2)/2$ and $\Delta\mathbf{r}\equiv\mathbf{r}_1-\mathbf{r}_2$, where $\mathbf{r}_1$ and $\mathbf{r}_2$ are the positions of the electron and hole, respectively. The vector $\mathbf{k}$ plays the role of the total momentum of the particles.[18,26,27] These wave functions were first derived by Lerner and Lozovik.[27] One can define a dipole moment of the exciton,

$$e\langle\psi_{\mathbf{k}n}|\Delta\mathbf{r}|\psi_{\mathbf{k}n}\rangle=el_0^2\mathbf{k}\times\hat{\mathbf{z}}\ , \tag{3.2}$$

which is perpendicular to $\mathbf{k}$ and proportional to k, independent of n.

In our earlier paper we calculated the exciton dispersion relations $E(\mathbf{k})$, which are exact to order $e^2/\epsilon l_0$ (i.e., in large magnetic fields). For filling factors $\nu=1$ (spin-polarized sample) and $\nu=2n$, $n=1,2,3,\ldots$ (both spins present in the highest occupied Landau level n), there is a single magnetoplasma mode near ω_c, and the dependence of the corresponding wave function on the positions of the electron and hole are just given by Eq. (3.1). The explicit expressions for the exciton energy, for $\nu=1$ and $\nu=2$, are[18,24]

$$E(\mathbf{k})=\omega_c+\frac{e^2}{2\epsilon l_0}\left\{\left[\frac{\pi}{2}\right]^{1/2}\left[1-e^{-k^2l_0^2/4}\left[(1+k^2l_0^2/2)I_0(k^2l_0^2/4)-\frac{k^2l_0^2}{2}I_1(k^2l_0^2/4)\right]\right]+\nu kl_0e^{-k^2l_0^2/2}\right\}, \tag{3.3}$$

where I_n is a modified Bessel function. For filling factor $\nu=2n+1$, $n=1,2,3,\ldots$, there are two modes near ω_c since an electron with spin down can be excited from Landau level n to $n+1$, or an electron with spin up from level $n-1$ to n. Exchange terms in the Coulomb interaction mix these two excitations, and the magnetoplasma modes are found by diagonalizing a 2×2 matrix. For $\nu=3$ the result is[18]

$$E^{\pm}(\mathbf{k})=\omega_c+\frac{E_{01}(\mathbf{k})+E_{12}(\mathbf{k})}{2}\pm\left[\left[\frac{E_{01}(\mathbf{k})+E_{12}(\mathbf{k})}{2}\right]^2+V_3(\mathbf{k})\right]^{1/2}, \tag{3.4}$$

where $E_{01}(\mathbf{k})\equiv E_{\nu=1}(\mathbf{k})-\omega_c$, as given by Eq. (3.3),

$$E_{12}(\mathbf{k})=\frac{e^2}{16\epsilon l_0}\left[\left[\frac{\pi}{2}\right]^{1/2}\{7-e^{-k^2l_0^2/4}[(7+\tfrac{9}{2}k^2l_0^2-2k^4l_0^4+k^6l_0^6/2)\times I_0(k^2l_0^2/4)-(\tfrac{7}{2}k^2l_0^2-k^4l_0^4+k^6l_0^6/2)I_1(k^2l_0^2/4)]\}+\frac{kl_0}{4}e^{-k^2l_0^2/2}(2-k^2l_0^2/2)^2\right], \tag{3.5}$$

and the off-diagonal matrix element is

$$V_3(\mathbf{k})=\frac{e^2}{\epsilon l_0}\frac{1}{\sqrt{8}}kl_0e^{-k^2l_0^2/2}(2-k^2l_0^2/2)\ . \tag{3.6}$$

These three dispersion curves are shown in Fig. 1. Similar expressions can be calculated for larger filling factors, but, since we are interested in the strong-magnetic-field limit, we will concentrate on the lowest filling factors, $\nu\leq 3$.

B. Density response function

The exciton dispersion curves correspond to poles in the density response function, which is defined as

$$\chi_{\text{pure}}(\mathbf{k},\omega)=-i\int_0^\infty dt\, e^{i\omega t}\langle[\rho_{\mathbf{k}}(t),\rho_{-\mathbf{k}}(0)]\rangle\ , \tag{3.7}$$

where the electron-density operator is

$$\rho_{\mathbf{k}}(t)=e^{i\mathcal{H}t}\sum_j e^{i\mathbf{k}\cdot\mathbf{r}_j}e^{-i\mathcal{H}t}\ .$$

[Here we are considering $\mathcal{H}=\mathcal{H}_0+\mathcal{H}_{e\text{-}e}$ from Eqs. (2.1b) and (2.1c).] In general, the form of $\chi_{\text{pure}}(\mathbf{k},\omega)$ is very complicated, even in the strong-field limit. However, we only need the terms $\chi^s_{\text{pure}}(\mathbf{k},\omega)$ which are singular near ω_c. For $\nu=1$ and $\nu=2$, these are[18]

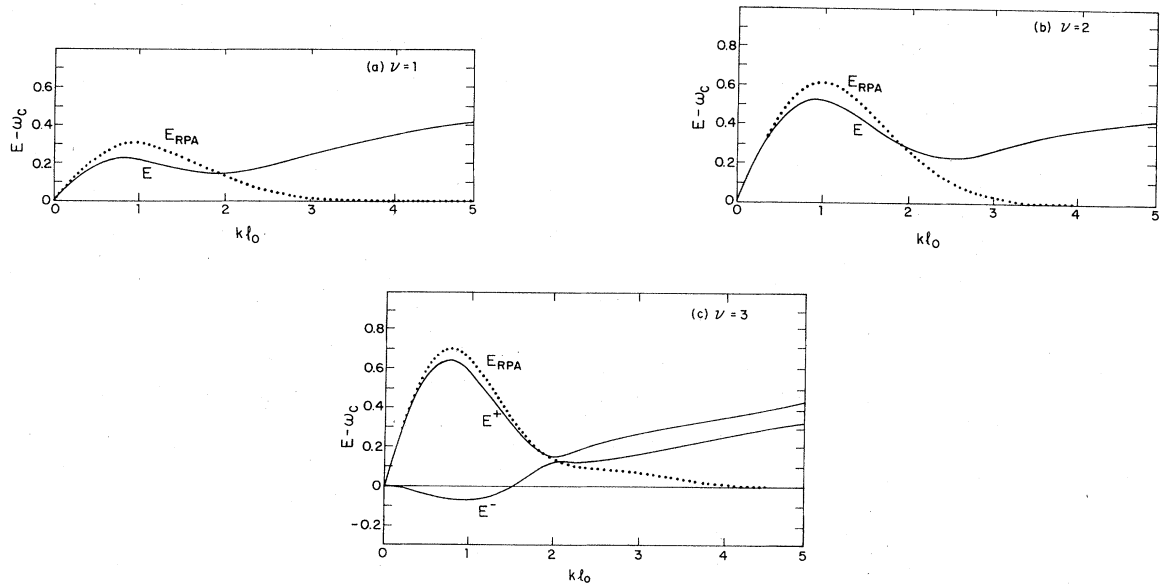

FIG. 1. Exciton dispersion curves near ω_c are shown for (a) $\nu=1$ (spin-polarized Landau level), (b) $\nu=2$ (both spins present in the lowest Landau level), and (c) $\nu=3$ (filled first Landau level and one spin state in second level). (These curves are from Ref. 18.) The energy scale is in units of $E_{\text{Co}}=e^2/\epsilon l_0$. The RPA energies are denoted by the dotted curves.

$$\chi^s_{\text{pure}}(\mathbf{k},\omega)=\frac{1}{2}\frac{k^2l_0^2e^{-k^2l_0^2/2}}{\omega-E(\mathbf{k})-i\epsilon}\ , \tag{3.8}$$

and, for $\nu=3$,

$$\chi^s_{\text{pure}}(\mathbf{k},\omega)=\tfrac{1}{4}k^2l_0^2e^{-k^2l_0^2/2}\left[\frac{2(\omega-E_{12})+(\omega-E_{10})(2-k^2l_0^2/2)^2-2\sqrt{2}\,V_3(2-k^2l_0^2/2)}{(\omega-E^+-i\epsilon)(\omega-E^--i\epsilon)}\right]. \tag{3.9}$$

IV. ABSORPTION TO LOWEST ORDER IN THE IMPURITY POTENTIAL

If the electron-impurity interaction $\mathscr{H}_{e\text{-}i}$ is treated as a small perturbation, one can expand the current-current correlation function of Eq. (2.5) to lowest order in the impurity potential U. One finds[9]

$$Q_+(\omega)=\frac{n_e e^2\omega_c/m^*}{\omega-\omega_c}+\frac{P(\omega)}{(\omega-\omega_c)^2}\ , \tag{4.1a}$$

$$P(\omega)=\frac{e^2}{2(m^*)2}n_I\sum_{\mathbf{k}}|U(\mathbf{k})|^2k^2 \times[\chi_{\text{pure}}(\mathbf{k},\omega)-\chi_{\text{pure}}(\mathbf{k},0)]\ , \tag{4.1b}$$

where n_I is the impurity concentration and $U(\mathbf{k})$ is the Fourier transform of the impurity potential. Here, $\chi_{\text{pure}}(\mathbf{k},\omega)$ is the density response function of the interacting electron gas without impurities. The thermal average in Eq. (3.7) is done in the *absence* of disorder.

Equations (2.4) and (4.1) give an expression for the conductivity which is valid to lowest order in the impurity concentration. The effect of impurities enters only through the factor $n_I|U(\mathbf{k})|^2$ in Eq. (4.1b). In principle, the effect of electron-electron interactions is treated exactly in this formalism, although, in practice, one may make some approximation for the density response function. However, this formalism does not include the effects of impurity-induced broadening of the excitations, and this may lead to spurious divergences in the absorption spectra.

Combining Eqs. (3.8) and (3.9) with Eqs. (2.4) and (4.1) gives an expression for the conductivity (near ω_c) which is valid for small disorder in the strong-field limit. The absorption is shown in Fig. 2 for $\nu=1$ and $\nu=3$, and short-range scattering, Eq. (2.3). Since the exciton dispersion curves have maxima and minima at finite wave vectors, and since there is no broadening due to electron-electron scattering for integer filling factors, there are inverse-square-root divergences in the density of exciton states at the energies of the maxima and minima. These divergences can be seen in the absorption spectra of Fig. 2. In addition, there is a $(\omega-\omega_c)^{-2}$ divergence in the $\nu=3$ spectra because of the lower branch of the magnetoplasma mode, which has energy ω_c at nonzero wave vector [see Fig. 2(c)].

In a proper self-consistent theory, the main peak at ω_c will be both broadened and shifted, and for realistic impurity potentials the extra structure at $\omega>\omega_c$ will have very small weight. [Recall that the amplitude of $P(\omega)$ scales with $n_I|U(\mathbf{k})|^2$ for weak impurity scattering.] Therefore it is difficult to draw any conclusions about the experimental line shape from this overly simplified theory.

V. ABSORPTION IN THE SELF-CONSISTENT EXCITON APPROXIMATION

A. Self-consistent exciton approximation

It is necessary to include higher-order effects of electron-impurity scattering to broaden the unphysical

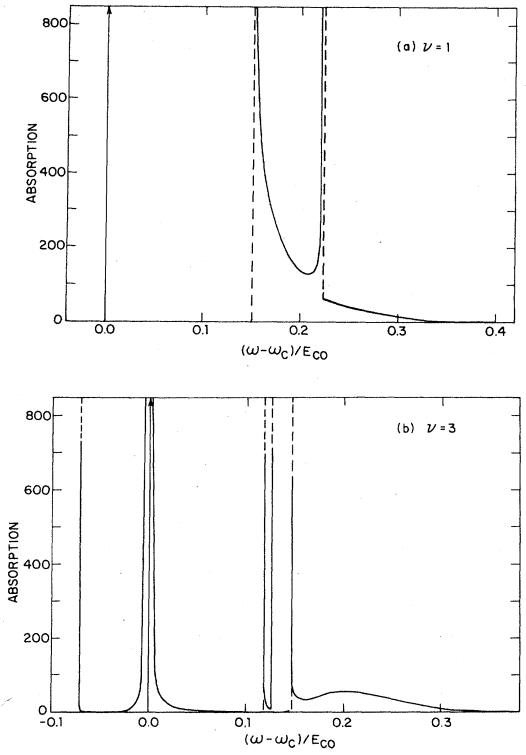

FIG. 2. Absorption near ω_c to lowest order in the impurity potential is shown for short-range scattering, and (a) $\nu=1$ (one spin-polarized Landau level), and (b) $\nu=3$. The vertical axes are $\text{Im}[D(0,\omega)]E_{\text{Co}}/U_2$, where $E_{\text{Co}}=e^2/\epsilon l_0$. There is a δ function at $\omega=\omega_c$, and the vertical dashed lines denote inverse-square-root edges. The absorption in the region $0<\omega-\omega_c<0.15E_{\text{Co}}$, for $\nu=1$, is nonzero, but cannot be seen on this scale. For $\nu=3$ there is also a $(\omega-\omega_c)^{-2}$ divergence because of the lower exciton mode.

divergences which are present in the lowest-order analysis of the preceding section. In this section we calculate the impurity-induced absorption, for the interacting system, by treating the impurity scattering in a self-consistent approximation. In the absence of disorder, all the neutral excitations of this system near ω_c are bound states of an electron and a hole, i.e., excitons. We use the exciton wave functions and energies of Sec. III and consider the scattering of excitons by impurities. The approximation, referred to as the SCEA, that we use for the exciton-impurity scattering is shown diagrammatically in Fig. 3.[25] The propagators are two-particle (electron-hole) propagators. The impurity can scatter either the electron or the hole—so that this approximation includes both self-energy and vertex corrections, much like the SCBA.[2] It differs from the SCBA, however, in that when the Coulomb potential is set equal to zero, some "crossed" diagrams [such as Fig. 4(a)] are included in the SCEA (because they are *not* crossed in the exciton basis). On the other hand, the diagram shown in Fig. 4(b) is included in the SCBA but not in the SCEA. (In the exciton basis, the impurity lines interfere.)

In the long-wavelength limit the excitons are tightly bound. Therefore, if the long-wavelength excitations are important in cyclotron absorption (as one may expect for GaAs, where the impurity potential is very long ranged), it is likely to be a good approximation to treat the excitons as a composite particle, and include impurity scattering to a given order in the exciton basis.

B. $\nu=1$ and $\nu=2$

For $\nu=1$ and $\nu=2$ there is only a single exciton mode near ω_c, and the exciton Green's function is a scalar. In the absence of disorder, the Green's function is

$$D_0(\mathbf{k},\omega)=\frac{1}{\omega-E(\mathbf{k})-i\epsilon}\ , \tag{5.1}$$

where the exciton energies $E(\mathbf{k})$ are given in Eq. (3.3).

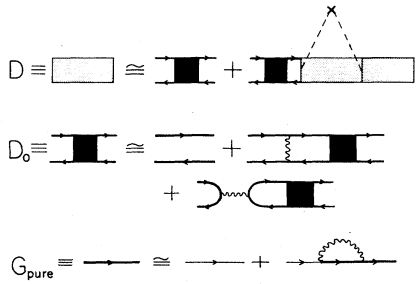

FIG. 3. Self-consistent exciton approximation for the two-particle Green's function $D(\mathbf{k},\omega)$ is shown. $D_0(\mathbf{k},\omega)$ is the two-particle Green's function in the absence of impurity scattering. The dashed lines denote the electron-impurity interaction (with the cross denoting the position of the impurity) and the wiggly lines denote the unscreened electron-electron interaction. The lines with arrows denote the single-particle Green's functions $G^0_{\rm pure}$ and $G_{\rm pure}$ of the noninteracting (thin lines) and interacting (thick lines) systems without impurities. The density response function of the pure system $\chi_{\rm pure}$ is simply related to D_0.

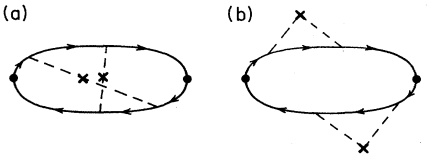

FIG. 4. Examples of diagrams which are included (a) in the self-consistent exciton approximation (SCEA) but not in the SCBA, and (b) in the SCBA but not in the SCEA, are shown for noninteracting electrons. The dashed lines denote the electron-impurity interaction and the crosses represent an impurity. Vertices are time ordered along horizontal axes. The SCBA is the self-consistent Born approximation commonly employed for noninteracting electrons.

The excitons "see" an effective impurity potential given by

$$\tilde{U}_I(\mathbf{r}_1,\mathbf{r}_2)=\sum_j [u(\mathbf{r}_1-\mathbf{R}_j,Z_j)-u(\mathbf{r}_2-\mathbf{R}_j,Z_j)] \tag{5.2a}$$

$$=\int \frac{d^2q}{(2\pi)^2}U_I(\mathbf{q})(e^{i\mathbf{q}\cdot\mathbf{r}_1}-e^{i\mathbf{q}\cdot\mathbf{r}_2})\ , \tag{5.2b}$$

where $\mathbf{r}_1$ and $\mathbf{r}_2$ are the positions of the electron and hole, respectively. $U_I(\mathbf{q})$ is the two-dimensional Fourier transform of the electron-impurity potential:

$$U_I(\mathbf{q})=\sum_j e^{i\mathbf{q}\cdot\mathbf{R}_j}\int d^2r\, u(\mathbf{r},Z_j)e^{i\mathbf{q}\cdot\mathbf{r}}\ . \tag{5.3}$$

In the presence of impurities, the Green's function D is written as

$$D^{-1}(\mathbf{k},\omega)=D_0^{-1}(\mathbf{r},\omega)-\Pi(\mathbf{k},\omega)\ . \tag{5.4}$$

In the SCEA the exciton self-energy Π satisfies the integral equation

$$\Pi(\mathbf{k},\omega)=n_I\int \frac{d^2q}{(2\pi)^2}\,|U(\mathbf{k}-\mathbf{q})|^2\,|M(\mathbf{k},\mathbf{q})|^2 D(\mathbf{q},\omega)\ , \tag{5.5}$$

where $U(\mathbf{q})$ is related to the configuration average of the impurity potential:

$$\langle U_I(\mathbf{q})U_I(-\mathbf{q}')\rangle_c\equiv n_I\,|U(\mathbf{q})|^2(2\pi)^2\delta(\mathbf{q}-\mathbf{q}')\ , \tag{5.6}$$

and n_I is the areal density of impurities. The matrix element M is defined by

$$\langle\Psi_{\mathbf{k}1}|e^{i\mathbf{q}\cdot\mathbf{r}_1}-e^{i\mathbf{q}\cdot\mathbf{r}_2}|\Psi_{\mathbf{q}'1}\rangle \equiv(2\pi)^2\delta(\mathbf{k}-\mathbf{q}-\mathbf{q}')M(\mathbf{k},\mathbf{k}-\mathbf{q})\ , \tag{5.7}$$

where the exciton wave function $\Psi_{\mathbf{k}1}(\mathbf{r}_1,\mathbf{r}_2)$ is defined in Eq. (3.1). The explicit form of the matrix element is

$$M(\mathbf{k},\mathbf{k}-\mathbf{q})=e^{-q^2l_0^2/4}[e^{i\mathbf{k}\times\mathbf{q}\cdot\hat{\mathbf{z}}l_0^2/2} -(1-q^2l_0^2/2)e^{-i\mathbf{k}\times\mathbf{q}\cdot\hat{\mathbf{z}}l_0^2/2}]\ . \tag{5.8}$$

Equations (5.1), (5.4), and (5.5) define the exciton Green's function D in the SCEA. The conductivity is simply related to the exciton Green's function by

$$\mathrm{Re}[\sigma_+(\omega)]=\frac{n_e}{\omega}\,|\langle n+1\,|\,j_+\,|\,n\rangle|^2\,\mathrm{Im}[D(0,\omega)] \tag{5.9a}$$

$$=\frac{n_e e^2\omega_c}{m^*\omega}(n+1)\mathrm{Im}[D(0,\omega)]\,, \tag{5.9b}$$

where n is the highest occupied Landau level ($n=0$ for $\nu=1$ and $\nu=2$), and $\langle n+1\,|\,j_+\,|\,n\rangle$ is the matrix element of the current operator $j_+=(j_x+ij_y)/\sqrt{2}$ between the nth and $(n+1)$th Landau level.

C. $\nu=3$

For filling factors $\nu=2n+1$, $n=1,2,3,\ldots$, there are two exciton modes near ω_c and the exciton Green's function is a 2×2 matrix. For $\nu=3$ the equations which define the Green's function are

$$D^{-1}_{\alpha\beta}(\mathbf{k},\omega)=D^{-1}_{0\alpha\beta}(\mathbf{k},\omega)-\Pi_{\alpha\beta}(\mathbf{k},\omega)\,, \tag{5.10}$$

$$\Pi_{\alpha\beta}(\mathbf{k},\omega)=n_I\sum_{\gamma,\delta}\int\frac{d^2q}{(2\pi)^2}\,|U(\mathbf{k}-\mathbf{q})|^2 M_{\alpha\gamma}(\mathbf{k},\mathbf{q})\times D_{\gamma\delta}(\mathbf{q},\omega)M^*_{\delta\beta}(\mathbf{k},\mathbf{q})\,, \tag{5.11}$$

where $\alpha,\beta=1,2$. In the basis in which the matrix elements are diagonal, one has[18]

$$D_0^{-1}(\mathbf{k},\omega)=\begin{bmatrix}\omega-\omega_c-E_{01}(\mathbf{k}) & -V_3(\mathbf{k})\\ -V_3(\mathbf{k}) & \omega-\omega_c-E_{12}(\mathbf{k})\end{bmatrix}, \tag{5.12}$$

where the energies E_{01}, E_{12}, and V_3 are defined in Sec. III B. The matrix elements are

$$(2\pi)^2\delta(\mathbf{k}-\mathbf{q}-\mathbf{q}')M(\mathbf{k},\mathbf{k}-\mathbf{q})=\begin{bmatrix}\langle\Psi_{k1}\,|\,e^{i\mathbf{q}\cdot\mathbf{r}_1}-e^{i\mathbf{q}\cdot\mathbf{r}_2}\,|\,\Psi_{q'1}\rangle & 0\\ 0 & \langle\Psi_{k2}\,|\,e^{i\mathbf{q}\cdot\mathbf{r}_1}-e^{i\mathbf{q}\cdot\mathbf{r}_2}\,|\,\Psi'_{q2}\rangle\end{bmatrix}, \tag{5.13}$$

where M_{11} is given by Eq. (5.8), and

$$M_{22}(\mathbf{k},\mathbf{k}-\mathbf{q})=e^{-q^2l_0^2/4}[(1-q^2l_0^2/2)e^{i\mathbf{k}\times\mathbf{q}\cdot\hat{\mathbf{z}}l_0^2/2}-(1-q^2l_0^2+q^4l_0^4/8)e^{-i\mathbf{k}\times\mathbf{q}\cdot\hat{\mathbf{z}}l_0^2/2}]\,. \tag{5.14}$$

VI. RESULTS

The integral equations of Eqs. (5.5) and (5.11) were solved by numerical iteration. In order to handle the poles correctly, the integrand was approximated piecewise as a ratio of quadratic polynomials and integrated analytically. There were no serious problems with convergence. When necessary, the value of the self-energy Π, obtained by an iteration, was mixed with its value on the previous iteration, to damp out oscillations. In general, convergence to $<1\%$ was obtained within 10 iterations. Three different impurity potentials were considered—short-range scatterers, long-range Coulomb scatterers as in GaAs heterojunctions, and an intermediate model. The results for these three potentials are discussed below.

A. Short-range scatterers

We first consider the simple case of short-range scatterers described by the potential of Eq. (2.3). The impurity potential enters the calculation of the conductivity, in our approximation, only in the form $n_I\,|\,U(\mathbf{q})\,|^2$, which is defined in Eq. (5.6), and is independent of $\mathbf{q}$ for short-range scatterers. This quantity can be related to the mobility μ in zero magnetic field by[2]

$$n_I\,|\,U(\mathbf{q})\,|^2=\frac{\hbar^3 e}{m^{*2}\mu}\,. \tag{6.1}$$

In units of the Coulomb energy $e^2/\epsilon l_0$, the impurity potential is characterized by the dimensionless parameter

$$U_2\equiv\frac{n_I\,|\,U(\mathbf{q})\,|^2/2\pi l_0^2}{(e^2/\epsilon l_0)^2}=\frac{\hbar^3\epsilon^2}{2\pi m^{*2}e^3\mu}\,. \tag{6.2}$$

The absorption near ω_c for $U_2=0.0025$, which corresponds to a mobility of 7.3×10^4 cm^2/V s, is shown in Fig. 5 for the case of a single filled Landau level ($\nu=1$). The somewhat surprising result is that the δ-function response at ω_c is shifted to $\omega_c^*<\omega_c$ (i.e., the effective mass is increased) but is not broadened. In addition, there is a broad peak at $\omega>\omega_c$, which is the self-consistent analog of the structure at $\omega>\omega_c$ in Fig. 2(a). For $U_2=0.0025$, about 15% of the total weight is in this second peak. However, since this peak is very broad ($\sim0.2e^2/\epsilon l_0$, where $e^2/\epsilon l_0=170$ K$=118$ cm^{-1} at 100 kG), one would not expect to see it with the sensitivity which is presently available in cyclotron resonance experiments. In any case, such a peak will not occur in the more realistic case of long-range scattering that is treated in the next section.

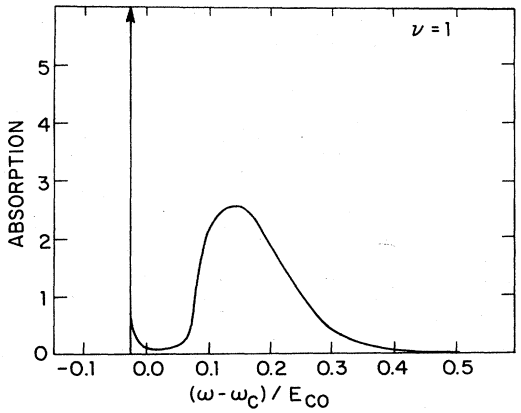

FIG. 5. The absorption, $E_{\mathrm{Co}}\mathrm{Im}[D(0,\omega)]$, near ω_c, is shown for $\nu=1$ and short-range scatterers. The dimensionless coupling constant is $U_2=0.0025$, which corresponds to a mobility of 7.3×10^4 cm^2/V s. About 85% of the weight is in the δ function at $\omega_c^*=\omega_c-0.025E_{\mathrm{Co}}$.

The intensity of this peak depends on the amplitude of large-momentum-transfer scattering, which is suppressed for long-range scatterers.

The absorption spectra for filling factors $\nu=1$ and $\nu=2$, and for other values of U_2, are qualitatively the same as those of Fig. 5. As U_2 increases, the shift of the δ function increases linearly and the weight of the secondary peak increases. (The weight of the δ function decreases by the same amount, of course, since the total weight obeys a sum rule.) It is possible that the δ function disappears or is broadened at some large but finite value of U_2. We have not studied values of U_2 larger than 0.01 in any detail because they correspond to very small mobilities and cyclotron effective masses much larger than those observed.

The fact that the resonance line is not broadened, in the SCEA, is a result of electron-electron interactions. In Fig. 6 we show the results for the noninteracting system ($e^2=0$), using the same approximation for impurity scattering. The results for the SCBA,[2] which is a more appropriate approximation for this limit, are also shown, as the dashed curve in Fig. 6. We display the results for $e^2=0$ to show the difference between the interacting and noninteracting cases. For $e^2=0$ there is a broad line which is symmetric about ω_c with a width $\Gamma \propto |U|$. (This symmetry will occur in any approximation that neglects both the electron-electron interaction and Landau-level mixing.)

We may now ask why the resonance line is unbroadened in the interacting system, for small values of U_2. If we examine the exciton Green's function $D(\mathbf{k},\omega)$, it appears that there is no broadening of the pole in the limit $k\to 0$ because the density of exciton states is small near the bottom of the band, and because the scattering matrix element $U(\mathbf{k}-\mathbf{q})M(\mathbf{k},\mathbf{q})$ vanishes rapidly, for $k\to 0$ and $q\to 0$, for short-range scatterers. In the SCEA the lowest-energy mode, which remains at $k=0$, is shifted to a frequency ω_c^*, which is lower than ω_c, and, for all k, the imaginary part of the self-energy $\Pi(\mathbf{k},\omega)$ is nonzero only for $\omega>\omega_c^*$.

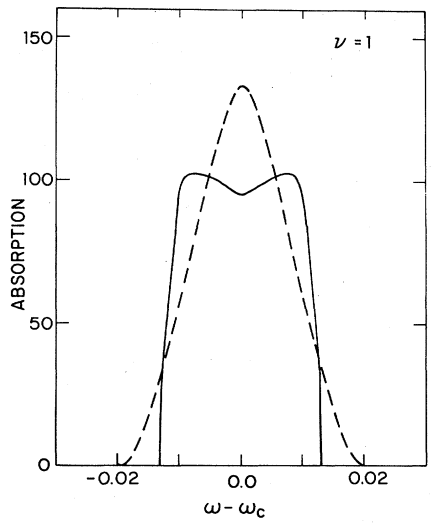

FIG. 6. Infrared absorption for the noninteracting system is shown for $\nu=1$ in the SCEA (solid curve) and SCBA (dashed curve) for short-range scatterers. The unit of energy is $20\,|U(q)|\,(n_I/2\pi l_0^2)^{1/2}$ to facilitate comparison with Fig. 5.

If one were to go beyond the SCEA and perform an exact analysis of the problem, one would find, even for short-range scatterers, that there is *some* broadening of the cyclotron mode at ω_c^*. For example, fluctuations of the impurity potential can localize short-wavelength excitons, resulting in a small density of localized excitons below ω_c^*. Then, mixing by the impurity potential of the localized states and the extended state at $k=0$ will result in a small width of the cyclotron line. One can estimate the density of the exciton states at threshold by using the analysis of Halperin and Lax.[28] One finds that the density of states at ω_c^* is proportional to $e^{-\gamma/U_2}$, where $\gamma\approx 0.1$ if one assumes that the largest contribution comes from the maxima and minima in the exciton dispersion curve. This is obviously a nonperturbative result and appears to give a very small broadening, since U_2/γ is small. Other possible broadening mechanisms are magnetic field inhomogeneities, thermal broadening, and higher-order electron-electron—interaction effects. All of these are expected to be small.

The absorption for filling factor $\nu=3$ is somewhat different. There are *two* poles (since the Green's function is a 2×2 matrix)—one of which is very narrow and has most of the weight. The cyclotron mode is broadened because of the lower branch of the magnetoplasma mode that crosses the ω_c axis at finite q [see Fig. 1(c)]. However, this broadening is very small ($\Gamma\sim 0.0008E_{\mathrm{Co}}$ at $\mu=7\times 10^4$ cm^2/V s), so the $\nu=3$ curve looks similar to the $\nu=1$ and $\nu=2$ curves.

Short-range scattering gives rise to a rather distinctive absorption spectrum—the dominant feature is a very narrow peak containing most of the weight. We believe that the fact that such a spectrum is not observed in GaAs heterojunctions is evidence of the importance of long-range scattering in these devices, as will be discussed in the next section.

B. Long-range scatterers

For filled Landau levels in GaAs-AlGaAs heterojunctions, the electrons interact with the ionized impurities in the AlGaAs through the unscreened Coulomb potential of Eq. (2.2). The two-dimensional Fourier transform of this potential is

$$u(\mathbf{q})=\frac{2\pi e^2}{\epsilon q}e^{i\mathbf{q}\cdot\mathbf{R}_i}e^{-qZ_i}. \tag{6.3}$$

(We neglect the difference in the dielectric constants of GaAs and AlGaAs.) If the impurities are uniformly ionized in a layer of thickness t, which is set back from the electron layer by a distance α, as shown in Fig. 7, the configuration average of Eq. (5.10) is

$$n_I\,|U(\mathbf{q})|^2=n_I\left[\frac{2\pi e^2}{\epsilon}\right]^2\frac{e^{-2\alpha q}}{q^2}\left[\frac{1-e^{-2tq}}{2tq}\right]. \tag{6.4}$$

For the case of long-range Coulomb scatterers, we define the dimensionless parameter

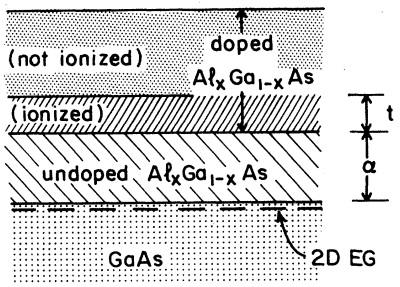

FIG. 7. Schematic drawing of a GaAs-AlGaAs heterojunction. The AlGaAs is modulation-doped with silicon. (Typical doping concentrations are about 10^{18} cm^{-2}.) We assume that the silicon is uniformly ionized in a layer of thickness t. The setback distance of the doped layer is α.

$$U_2 \equiv \left[\frac{n_I}{2\pi}\left[\frac{2\pi e^2}{\epsilon}\right]^2\right] \Big/ \left[\frac{e^2}{\epsilon l_0}\right]^2 = 2\pi l_0^2 n_I \ . \tag{6.5}$$

The concentration of ionized impurities n_I can be treated as a parameter which is fixed by the desired mobility. However, by assuming that all the scattering is due to ionized impurities, one can calculate mobilities in good agreement with experiment.[29,30] Following the analysis of Ando,[29] we assume that there are both donor and acceptor impurities with a fixed ratio,

$$n_I \approx \tfrac{5}{3} n_e \ , \tag{6.6}$$

where n_e is the density of electrons in the inversion layer.

For a given setback α, thickness t, and electron density n_e, the mobility can be calculated from the expression

$$\frac{1}{\mu} = \frac{2m^2}{e\hbar^3}\int_0^\pi \frac{d\theta}{\pi} n_I \, |\, U_s(2k_F \sin\theta)\,|^2 \sin^2\theta \ , \tag{6.7}$$

where the Fermi wave vector is $k_F = (2\pi n_e)^{1/2}$. Since the

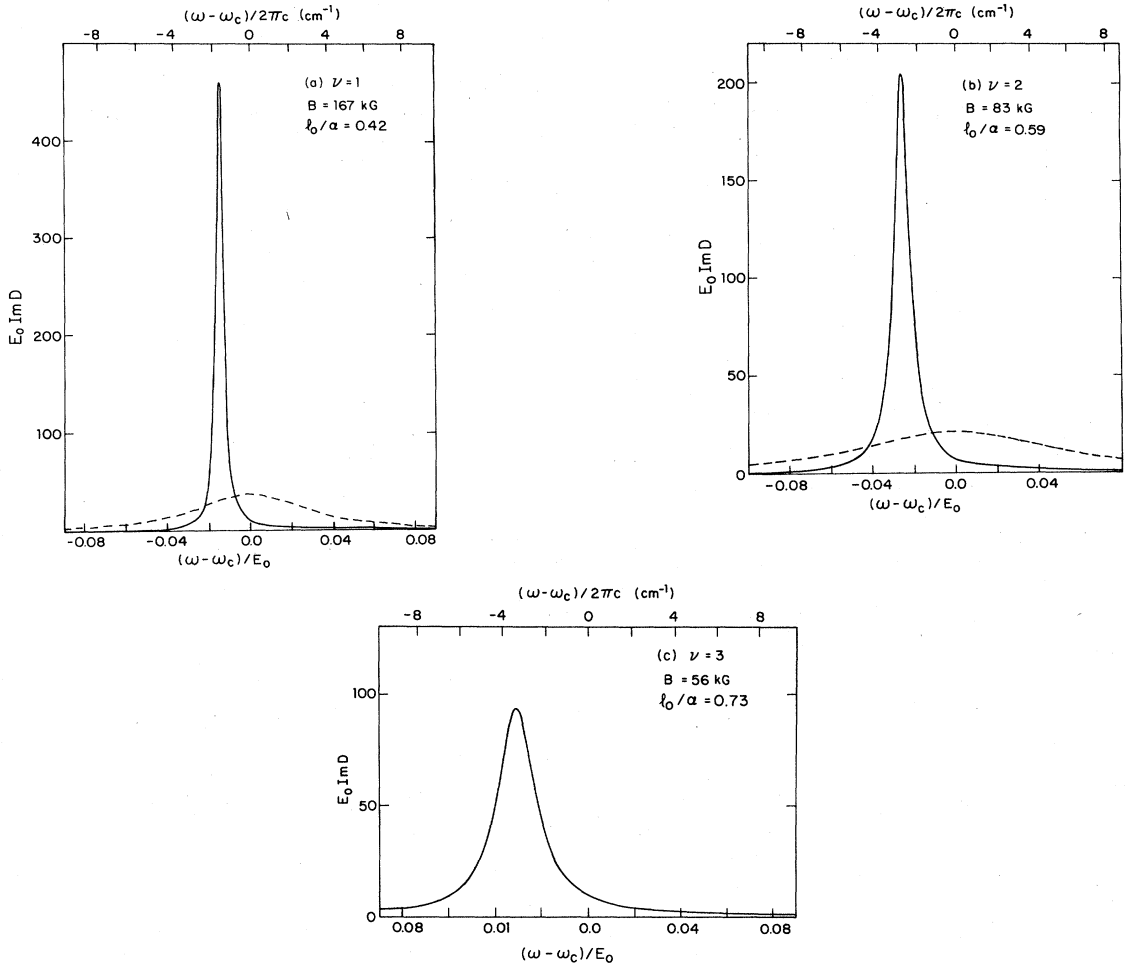

FIG. 8. Infrared absorption, $E_0\mathrm{Im}[D(0,\omega)]$, near ω_c, is shown for long-range scatterers and filling factors (a) $\nu=1$, (b) $\nu=2$, and (c) $\nu=3$. The electron density is 4×10^{11} cm^{-2}, the impurity setback α is 150 Å, the thickness of the ionized-impurity layer t is 100 Å, and the energy $E_0 \equiv (\pi n_e)^{1/2}(e^2/\epsilon) = 155$ K (108 cm^{-1}) in all three cases. The dimensionless coupling constant U_2 was chosen to correspond to a mobility of 2.7×10^5 cm^2/V s. Frequency shifts are marked in units of cm^{-1} on the upper scale, and the full widths at half maximum (FWHM), in cm^{-1}, are (a) 0.6, (b) 1.0, and (c) 1.9. The absorptions in the SCEA for the noninteracting system are also shown (dashed lines).

mobility is a zero-magnetic-field property, it is the statically *screened* impurity potential,[31]

$$|U_s(\mathbf{q})|^2 \approx \left[\frac{2\pi e^2}{\epsilon}\right]^2 \frac{e^{-2\alpha q}}{(q+q_{\rm TF})^2}\left[\frac{1-e^{-2tq}}{2tq}\right], \quad (6.8)$$

which enters the expression for the mobility. The Thomas-Fermi wave vector, here, is $q_{\rm TF}=2m^*e^2/\epsilon\hbar^2$.

For fixed t and n_e, one can vary the mobility by varying the setback α. For a given filling factor, the electron density also determines the magnetic field. Since we are interested in the strong-field limit, we consider a moderately high electron density, $n_e=4\times10^{11}$ cm^{-2}, which is typically achieved at setbacks $\alpha\leq 200$ Å. We take the thickness t to be 100 Å, which we believe is a reasonable value for typical devices. For $t=100$ Å and $n_e=4\times10^{11}$ cm^{-2}, we have studied the cases $\nu=1$, 2, and 3 for setbacks $100\leq\alpha\leq 200$ Å. Some typical results are shown in Fig. 8.

In all cases, for long-range scatterers, the peak of the cyclotron line is shifted to $\omega_c^*<\omega_c$ and broadened. The peak for $\nu=3$ has more weight at $\omega<\omega_c^*$ and is broader than those for $\nu=1$ and $\nu=2$ because of the lower branch of the magnetoplasma mode. From Eq. (5.9), the width of the cyclotron line is

$$\mathrm{Im}[\Pi(0,\omega_c^*)]=\left[\frac{e^2}{\epsilon l_0}\right]^2 U_2 l_0\int_0^\infty dq\, e^{-2\alpha q}\left[\frac{1-e^{-2tq}}{2tq}\right] \times q^3 l_0^3 e^{-q^2l_0^2/2}\mathrm{Im}[D(q,\omega_c^*)]\,. \quad (6.9)$$

The width comes mainly from intermediate wave vectors $ql_0\approx 1$, although the range of q that contributes is cut off for larger setbacks by the factor of $e^{-2\alpha q}$ in Eq. (6.9). The energy of the magnetoplasma mode, defined by $\mathrm{Re}[D^{-1}(\mathbf{q},\omega(\mathbf{q}))]=0$, and its width, $\mathrm{Im}[\Pi(\mathbf{q},\omega(\mathbf{q}))]$, in the SCEA, are shown in Fig. 9, as the solid and dashed curve, respectively. For long-range scatterers the broadening of the magnetoplasma mode is sufficiently great that, even within the SCEA, the Green's functions for $ql_0\approx 1$ have low-energy tails that overlap the energy ω_c^* of the $q=0$ exciton. The broadening is much larger than that for short-range scatterers at the same mobility, because long-range scattering is relatively ineffective in contributing to the transport scattering rate $1/\tau_t$, which is related to the mobility ($\mu=e\tau_t/m^*$). Therefore, for a given mobility, the dimensionless parameter U_2, which partly characterizes the strength of the potential, is much larger (typically several orders of magnitude larger) for long-range scatterers than for short-range scatterers. Although long-range scatterers do not contribute much to $1/\tau_t$, they do significantly broaden the cyclotron line.

In earlier work, Das Sarma and Stern[21] pointed out that long-range scatterers contribute significantly to the single-particle scattering rate $1/\tau_s$, such that $\tau_s\ll\tau_t$ (for typical setbacks), and, therefore, have a large effect on single-particle level broadening, even in high-mobility samples. In the present calculation, the cyclotron width $\Gamma_{\rm CR}$ is not simply related to either τ_t or τ_s. For example, if the carrier density is held fixed and only the setback distance is varied, we find that $1/\Gamma_{\rm CR}$ varies more rapidly than either τ_s or τ_t, for the range of parameters considered.

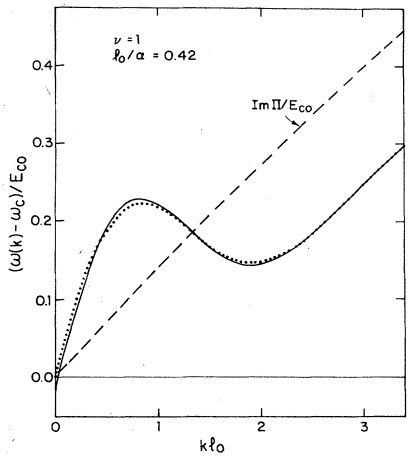

FIG. 9. Frequency and width of the magnetoplasma mode near ω_c are shown for long-range scatterers and $\nu=1$. The parameters used are the same as in Fig. 8(a). The solid curve is given by $\mathrm{Re}[D(q,\omega(q))]^{-1}=0$, and the dashed curve denotes the width $\mathrm{Im}[\Pi(q,\omega(q))]$. The magnetoplasma mode for the pure system (dotted curve) is also shown.

Several features of Fig. 9 are worth noting. One striking feature is that for values of $kl_0\geq 0.1$, the width of the exciton line, $\mathrm{Im}[\Pi(\mathbf{k},\omega)]$, is much greater than the frequency shift, $\mathrm{Re}\Pi$. Over the wave-vector range illustrated, $\mathrm{Im}\Pi$ increases roughly linearly with k, an effect which reflects the variation of the strength of the coupling of the exciton to the long-wavelength fluctuations of the impurity potential. We obtain a reasonable estimate of the linewidth by writing

$$\mathrm{Im}\Pi\approx ekl_0^2E_{\rm rms}\,, \quad (6.10)$$

where $E_{\rm rms}$ is the root-mean-square value of the electric field in the x-y plane arising from the random impurity potential, and ekl_0^2 is the electric dipole moment of the exciton.[18,27] When the electron-hole separation kl_0^2 becomes large compared to the setback distance α, one can no longer regard the electric field as constant over the area of the exciton, and one must integrate potential fluctuations over the wave vectors k' in the range $(kl_0^2)^{-1}<k'<\alpha^{-1}$ in order to calculate the mean-square potential difference between the electron and hole positions. This leads to a linewidth $\mathrm{Im}\Pi\propto(\ln k)^{1/2}$ for large values of k.

For the cyclotron resonance line, at $k=0$, we found that motion of the exciton, arising from the electron-electron interaction, gave a considerable narrowing of the line compared to the noninteracting case ($e^2=0$). [See Fig. 8(a).] For moderate values of kl_0, however, motional narrowing should be a much smaller effect because the effective impurity potential is stronger, while the exciton velocity is actually smaller. For large values of k we might expect a Gaussian shape to be a better approximation to the form of the exciton line than the form that would be obtained from our self-consistent exciton approximation.

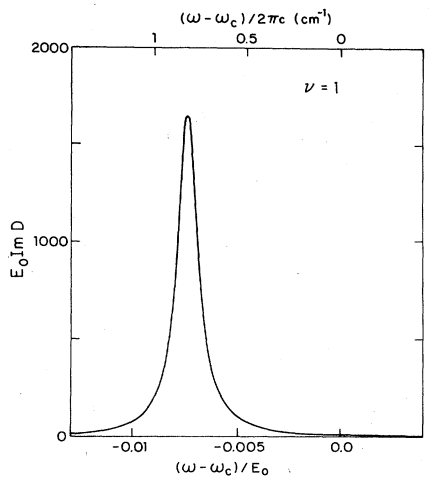

FIG. 10. Infrared absorption near ω_c for $\nu=1$ is shown for scattering from the potential of Eq. (6.11), with a length scale $b=150$ Å. For $n_e=4\times10^{11}$ cm^{-2}, the mobility is 10^5 cm^2/V s. The FWHM is 0.1 cm^{-1}.

For purposes of illustration, we have also considered a scattering potential whose configuration average has the form

$$n_I \mid U(q) \mid^2 = n_I C \frac{e^{-2bq}}{q} , \tag{6.11}$$

where b and C are constants. This potential was employed by Fukuyama, Kuramoto, and Platzman as a model for surface roughness.[21] We considered this potential because it is intermediate between long-range Coulomb scattering and short-range scattering. The absorption spectrum for $\nu=1$, $b=150$ Å, and $C=3.7$, which corresponds to a mobility of 10^5 cm^2/V s at $n_e=4\times10^{11}$ cm^{-2}, is shown in Fig. 10. Again, the curve is shifted to $\omega_c^* < \omega_c$ and broadened, but the width is smaller than that for Coulomb scattering at the same mobility.

VII. CONCLUSIONS

If one *neglects* electron-electron interactions, the linewidths calculated for realistic impurity potentials (long-range scatterers) in high-mobility GaAs heterojunctions are almost an order of magnitude larger than those measured in cyclotron resonance experiments. (For a mobility of 2×10^5 cm^{-2}/V s, the measured linewidth is about 1 cm^{-1} in strong magnetic fields.[14]) If one assumes that the scatterers are short ranged, then, neglecting electron-electron interactions, one does obtain linewidths in reasonable agreement with experiments. However, we believe such agreement is fortuitous since there will certainly be some long-range scattering from the ionized impurities. In fact, the mobility in GaAs heterojunctions has been observed to increase with electron density as $\mu \sim n_e^{1.65}$, implying that this long-range scattering is the dominant scattering mechanism.[18] We have shown that if one considers long-range scatterers and electron-electron interactions together, then one obtains linewidths in agreement with experiment. We believe that electron-electron interactions are important and must be considered not only for understanding "anomalies" in the cyclotron resonance, but also for understanding the shape of the main cyclotron peak in high-mobility GaAs heterostructures. Impurity scattering must be treated self-consistently, and one cannot replace the single-particle lifetime by the transport lifetime.[21]

In this paper we have treated electron-electron interactions and impurity scattering self-consistently by restricting ourselves to the case of filled Landau levels and strong magnetic fields. It should be noted that our results may not be directly applicable to current experiments because the parameter $e^2/\epsilon l_0 \omega_c$ is of order unity in most of the experiments. However, we do obtain linewidths and resonance frequency shifts which are in qualitative agreement with experiments that have been done on high-mobility GaAs heterojunctions in strong magnetic fields with $\nu \geq 1$.[14,32] The shift to lower frequencies arises naturally from considering the effect of impurity scattering on the $q=0$ exciton. It is the lowest-energy mode and is shifted down in energy as it is mixed with other modes by the impurity potential.

Our analysis offers no explanation for the anomalous linewidth broadening or splitting[12,14] at intermediate field strengths ($E_{\mathrm{Co}}/\omega_c \approx 1$) which has been attributed to electron-electron—interaction effects. In the model of Schlesinger *et al.*,[14] the cyclotron line is broadened or split when finite-wave-vector magnetoplasma modes are shifted into resonance with the cyclotron mode at $q=0$. Since this phenomenon is believed to be related to the electron density and not the filling factor, one can analyze their model in light of our results for integer fillings. For $\nu=1$ or 2, for example, one may be tempted to identify their "shift parameter" δ with the minimum of the exciton curve at $ql_0 \approx 2$. This minimum will be shifted to lower energies, as the magnetic field strength decreases, by higher-order corrections in E_{Co}/ω_c. At magnetic fields where this minimum lies close to ω_c, one might expect to see two peaks in the infrared-absorption spectra, from the model of Schlesinger *et al.* However, there are several problems with this possibility: (1) Some of the higher-order corrections to the exciton curve have been calculated by MacDonald[33] in the Hartree-Fock approximation, and the corrections for $E_{\mathrm{Co}}/\omega_c \leq 2$ are too small to bring the minimum into resonance with the cyclotron mode. (2) Even if the minimum did cross the ω_c axis, the sign of δ would appear to be inconsistent with the experimental data. The data suggest that at high fields there is a finite-wave-vector mode below ω_c which moves upward in energy as the magnetic field is decreased. (3) From our analysis, if the minimum is shifted to ω_c one would expect the second peak to be much broader than the main cyclotron peak. Experimentally, they see two peaks of comparable widths. In light of all this, it is difficult to imagine how coupling to finite-wave-vector magnetoplasma modes alone will explain the anomalous line splitting, at arbitrary filling factors. One may need to include other effects such as spin-dependent interactions, electron-phonon interactions,[34] other corrections to the high-field limit, or different impurity potentials.

We believe that it would be useful to have systematic

experimental measurements of cyclotron resonance of high-mobility heterojunctions at integer filling factors and in strong magnetic fields, where the theoretical simplifications made in the present analysis are applicable. Interpreting cyclotron resonance experiments is complicated by the fact that it is difficult to vary parameters independently. (In particular, it is difficult to vary the electron density in GaAs heterojunctions, while holding the impurity potential fixed, and vice versa.) Therefore it is useful to consider a limit where the effects that we know are important (in this case, electron-impurity scattering and electron-electron scattering) can be accurately calculated. In the simple case of filled Landau levels and very strong magnetic fields, one can calculate electron-electron—interaction effects exactly and can treat electron-impurity scattering self-consistently. (Even though the impurity potential may be very weak, it is insufficient to treat electron-impurity scattering to lowest order only, as this completely neglects the linewidth broadening due to electron-impurity scattering.) Since the absorption line shape depends strongly on the form of the impurity potential, comparison between theory and experiment, in this simple case, could tell one something about the impurity potential. Such comparison could also tell one what other effects (such as those mentioned above) are important in cyclotron resonance.

An experimental probe which is closely related to cyclotron resonance is resonant Raman scattering in the presence of strong magnetic fields. This probe has been used to investigate the behavior of electrons in the inversion layers of multi-quantum-well heterostructures[35] and, in principle, could also be used to study the two-dimensional system of a single heterojunction. Unlike cyclotron resonance experiments, magneto-Raman scattering directly probes finite wave vectors. The wave vector parallel to the surface is determined by the scattering angle and wavelength of the incident light, which is required to have an energy matched to the band gap of the semiconductor. In GaAs, in a magnetic field of 100 kG, one can study wave vectors in the range $0 < ql_0 < 0.2$. In addition, by looking at different polarizations of the incident and scattered light, one can change the selection rules and thus study different exciton branches. Although the present paper has concentrated on the theory of cyclotron resonance, i.e., the response at $q=0$, the response functions at finite wave vectors are also generated, in the self-consistent exciton approximation, by our iterative procedures. The most striking qualitative features of these results are that the linewidths of the various exciton branches increase rapidly with increasing wave vector, even for samples of high mobility, while the centers of the lines stay rather close to the exciton energies $E(q)$ for the system without impurity scattering. (See, for example, Fig. 9, and discussion thereof.)

ACKNOWLEDGMENTS

The authors are grateful for helpful conversations with Z. Schlesinger, A. J. Berlinsky, S. Das Sarma, P. A. Lee, P. M. Platzman, F. Stern, H. Stormer, J. Worlock, C. Perry, and H. Ehrenreich. This work was supported in part by the National Science Foundation under Grant No. DMR-82-07431. One of us (C.K.) acknowledges support from the National Science and Engineering Research Council of Canada, and has benefited from the hospitality of the Aspen Center for Physics during part of this work.

*Present address: Institute for Theoretical Physics, University of California, Santa Barbara, CA 93106.

[1]For a review of two-dimensional electron systems, see T. Ando, A. B. Fowler, and F. Stern, Rev. Mod. Phys. **54**, 437 (1981).

[2]T. Ando, J. Phys. Soc. Jpn. **38**, 989 (1975); **36**, 959 (1974); **37**, 1233 (1975).

[3]T. Ando, J. Phys. Soc. Jpn. **36**, 1521 (1974); **37**, 622 (1974).

[4]S. Fujita and M. Prasad, J. Phys. Chem. Solids **38**, 1351 (1977); M. Prasad and V. K. Arora, Surf. Sci. **113**, 333 (1982).

[5]W. Götze and J. Hajdu, Solid State Commun. **29**, 89 (1979).

[6]G. Abstreiter, J. F. Koch, P. Goy, and Y. Couder, Phys. Rev. B **14**, 2494 (1976).

[7]J. P. Kotthaus, G. Abstreiter, and J. F. Koch, Solid State Commun. **15**, 517 (1974).

[8]T. Ando, Phys. Rev. Lett. **36**, 1383 (1976).

[9]C. S. Ting, S. C. Ying, and J. J. Quinn, Phys. Rev. Lett. **37**, 215 (1976); Phys. Rev. B **16**, 5394 (1977).

[10]B. A. Wilson, S. J. Allen, Jr., and D. C. Tsui, Phys. Rev. Lett. **44**, 479 (1980); Phys. Rev. B **24**, 5887 (1981).

[11]K. Muro, S. Narita, S. Hiyamizu, K. Nanbu, and H. Hashimoto, Surf. Sci. **113**, 321 (1982).

[12]Th. Englert, J. C. Maan, Ch. Uihlein, D. C. Tsui, and A. C. Gossard, Solid State Commun. **46**, 545 (1983).

[13]S. Das Sarma, Solid State Commun. **36**, 357 (1980).

[14]Z. Schlesinger, S. J. Allen, J. C. M. Hwang, P. M. Platzman, and N. Tzoar, Phys. Rev. B **30**, 435 (1984).

[15]W. Kohn, Phys. Rev. **123**, 1242 (1961).

[16]W. Götze and P. Wölfle, Phys. Rev. B **6**, 1226 (1972).

[17]Y. Shiwa and A. Isihara, J. Phys. C **16**, 4853 (1983). See also A. Isihara and M. Jukai, Phys. Rev. B **24**, 7408 (1981).

[18]C. Kallin and B. I. Halperin, Phys. Rev. B **30**, 5655 (1984).

[19]M. A. Paalanen, D. C. Tsui, A. C. Gossard, and J. C. M. Hwang, Phys. Rev. B **29**, 6003 (1984).

[20]T. J. Drummond, H. Morkoç, K. Hess, and A. Y. Cho, J. Appl. Phys. **52**, 5231 (1981).

[21]S. Das Sarma and F. Stern (unpublished).

[22]H. Fukuyama, Y. Kuramoto, and P. M. Platzman, Phys. Rev. B **19**, 4980 (1979); Surf. Sci. **73**, 491 (1978).

[23]One cannot make a direct comparison between the analysis of Ref. 22 and the present work because the results of Ref. 22 are not well defined in the limit of zero temperature and integer filling factor, where our formulas apply.

[24]Yu. A. Bychkov, S. V. Iordanskii, and G. M. Éliashberg, Pis'ma Zh. Eksp. Teor. Fiz. **33**, 152 (1981) [JETP Lett. **33**, 143 (1981)].

[25]For an early use of this type of self-consistent approximation in the analysis of exciton propagation in a three-dimensional semiconductor, see the "$\Gamma=1$ approximation" of A. Suna [Phys. Rev. **135**, A111 (1964)].

[26]L. P. Gor'kov and I. E. Dzyaloshinksii, Zh. Eksp. Teor. Fiz. **53**, 717 (1967) [Sov. Phys.—JETP **26**, 449 (1968)].

[27]I. V. Lerner and Yu. E. Lozovik, Zh. Eksp. Teor. Fiz. **78**,

1167 (1978) [Sov. Phys.—JETP **51**, 588 (1980)].
[28]B. I. Halperin and M. Lax, Phys. Rev. **148**, 722 (1966); **153**, 802 (1967).
[29]T. Ando, J. Phys. Soc. Jpn. **51**, 3900 (1982).
[30]F. Stern, Appl. Phys. Lett. **43**, 974 (1983).
[31]F. Stern, Phys. Rev. Lett. **18**, 546 (1964).
[32]K. Muro, S. Mori, S. Narita, S. Hiyamizu, and K. Nanbu, Surf. Sci. **142**, 394 (1984).
[33]A. J. MacDonald, J. Phys. C (to be published)
[34]D. M. Larsen, Phys. Rev. B **30**, 4595 (1984).
[35]A. Petrou, C. H. Perry, M. C. Smith, J. M. Worlock, R. L. Aggarwal, A. C. Gossard, and W. Wiegmann (unpublished).